



Pressure drop caused by flow area changes in capillaries under low flow conditions

Toufik Y. Chalfi, S.M. Ghiaasiaan *

G.W. Woodruff School of Mechanical Engineering, Georgia Institute of Technology, Atlanta, GA 30332-0405, United States

Received 29 June 2007; received in revised form 20 September 2007

Abstract

Single-phase and two-phase flow pressure drops caused by flow area expansion and contraction were measured using air and water. The test section consisted of two capillaries with 0.84 mm and 1.6 mm diameters. For single-phase flow, the Reynolds numbers defined based on the smaller diameter capillary covered the range 160–11,000. For two-phase flow, the all-liquid Reynolds number based on the smaller capillary varied in the 410–1020 range, and the flow quality varied in the 0.018–0.2 range. The single-phase flow loss coefficients for both flow area expansion and contraction were empirically correlated. For two-phase flow, the data indicated the occurrence of significant velocity slip, and the one-dimensional homogeneous flow model utterly disagreed with the data. For flow area expansion the one-dimensional slip flow model along with an Armand-type slip ratio correlation could predict the data well. For flow area contraction, the one-dimensional slip flow model along with the slip ratio expression of Zivi agreed with the data very well, provided that no vena-contracta was considered.

© 2007 Elsevier Ltd. All rights reserved.

Keywords: Pressure drop; Expansion; Contraction; Single-phase; Two-phase; Microchannel

1. Introduction

Pressure losses caused by flow disturbances (minor pressure losses) are among the least studied aspects of flow in mini and microchannels. The literature dealing with this topic in common channels is relatively extensive (see review in Abdelall et al., 2005). The existing methods are unlikely to be applicable directly to mini and microchannels, however. These pressure losses are common in miniature head exchangers, as well as many experiments aimed at understanding two-phase flow in mini and microchannels, however miniature heat exchangers, evaporators and condensers are typically composed of an array of parallel mini or microchannels connected to common inlet and outlet plena. The pressure drop at the interface between the channels and the plena are important, in particular when significant phase change (boiling or condensation) occurs inside the channels. The dynamic coupling between the plena and the channels can indeed lead to flow oscillations

* Corresponding author. Tel.: +1 404 894 3746; fax: +1 404 894 8496.
E-mail address: mghiaasiaan@gatech.edu (S.M. Ghiaasiaan).

(Qu and Mudawar, 2004; Chen and Chang, 2005; Wu and Cheng, 2003). An understanding of the magnitude pressure losses at the channel/plenum interface is evidently important for the correct modeling of these systems. Pressure drops associated with abrupt flow area changes are also important for the correct interpretation of experimental data dealing with mini and microchannel hydrodynamic processes, because many experimental studies in the past have used test section connected to inlet and exit plena, or at least enlarged flow areas, and have measured pressures in these plena or enlarged sections. The common practice for the estimation of minor pressure drop in miniature systems has been to use commonly-applied macro-scale models and correlations, in particular the homogeneous flow model when two-phase flow is involved (Triplett et al., 1999; Bowers and Mudawar, 1994; Zhang and Webb, 2001). The separated flow model with slip ratio and vena-contracta contraction coefficient (in case of flow area contraction) parameters representative of macro-scale systems has also been applied (Yang and Webb, 1996; Zhang and Webb, 2001).

Little has been reported with respect to two-phase pressure drops caused by flow disturbances in mini and microchannels. Abdelall et al. (2005) conducted experiments with air and water, and measured pressure changes in the abrupt flow area expansion or contraction at the interface between two circular channels, one with an inner diameter of 1.6 mm, the other with an inner diameter of 0.84 mm. They made measurements with single-phase (gas or liquid) as well as two-phase flows, all at relatively high flow rates. Based on their smaller channel characteristics, the Reynolds number in their single-phase flow experiments covered the range $870\text{--}1.3 \times 10^4$. The two-phase, all-liquid Reynolds number in their experiments varied in the range $Re_{LO} = 1.75 \times 10^3\text{--}3.5 \times 10^3$, where $Re_{LO,1} = G_1 D_1 / \mu_L$. In the latter expression D_1 and G_1 represent the diameter and the total mass flux in the smaller channel, μ represents viscosity, and subscript L represents the liquid phase. Abdelall et al. noted that for both flow area expansion and contraction their data behaved differently than what commonly-applied macro-scale correlation predicted. The homogeneous flow model, in particular, lead to very significant overprediction of the pressure changes caused by flow area expansion or contraction. The data indeed indicate the occurrence of strong velocity slip, consistent with recent observation dealing with two-phase flow in mini and micro channels (Chung et al., 2004).

In this article we report on experiments dealing with pressure drop in abrupt flow area changes, at low flow rates. Thermal-hydraulic phenomena at low flow rates are common in miniature systems and are therefore of particular interest. The experiments were carried out using the test loop of Abdelall et al. (2005), with some modifications.

2. Experiments

Fig. 1 is a schematic of the test loop. Distilled water flow is provided by a rubber bladder within a steel tank, and compressed air originating from the building air supply system, passes through a filtered and regulated line. The air and water streams meet in the tee fitting upstream the test section after their flow rates are measured by a set of flow-meters. The tee fitting has an inner diameter of 4.8 mm, and 178 mm long.

The pressure drop measurement system included six pinholes of 0.5 mm diameter and located at 20 mm intervals serve as pressure taps for each of the two tubes. These clean and burr-free pinholes were created on the tube walls using precision electric discharge machining (EDM). A threaded hole with 8.6 mm diameter in the brass housing. The pressure taps “4” and “C” are located at 25 mm from the singularity. Details of the test section and pressure drop measurement system can be found in Abdelall et al. (2005).

The pressure measurements are done such that at any time only two pressure transducers are used, one for measuring the absolute pressure at pinhole 1, the other measuring the pressure difference in any of the other eleven stations. This arrangement eliminates cross-calibration errors. For this purpose, the pressure taps are connected to 7-way selector valve with 3.2 mm inner diameter plastic tubing, in turn the selector valve is connected to a 3-way selector valve. The latter 3-way valve is connected to a differential pressure transducer. Table 1 is a summary of the measurement instrument accuracies.

Single-phase flow tests with air were initiated by first making sure that all the system was dry, and in single-phase flow tests with water it was first verified that no trapped air bubbles were present. Each two-phase test was initiated by first verifying that all tubing lines were full of water. The gas and liquid flow rates were then adjusted. The pressure drop between adjacent pressure tap pairs were then measured, and the steady-state pressure profiles similar to those displayed in Figs. 2 and 3 were plotted. The pressure change across the flow

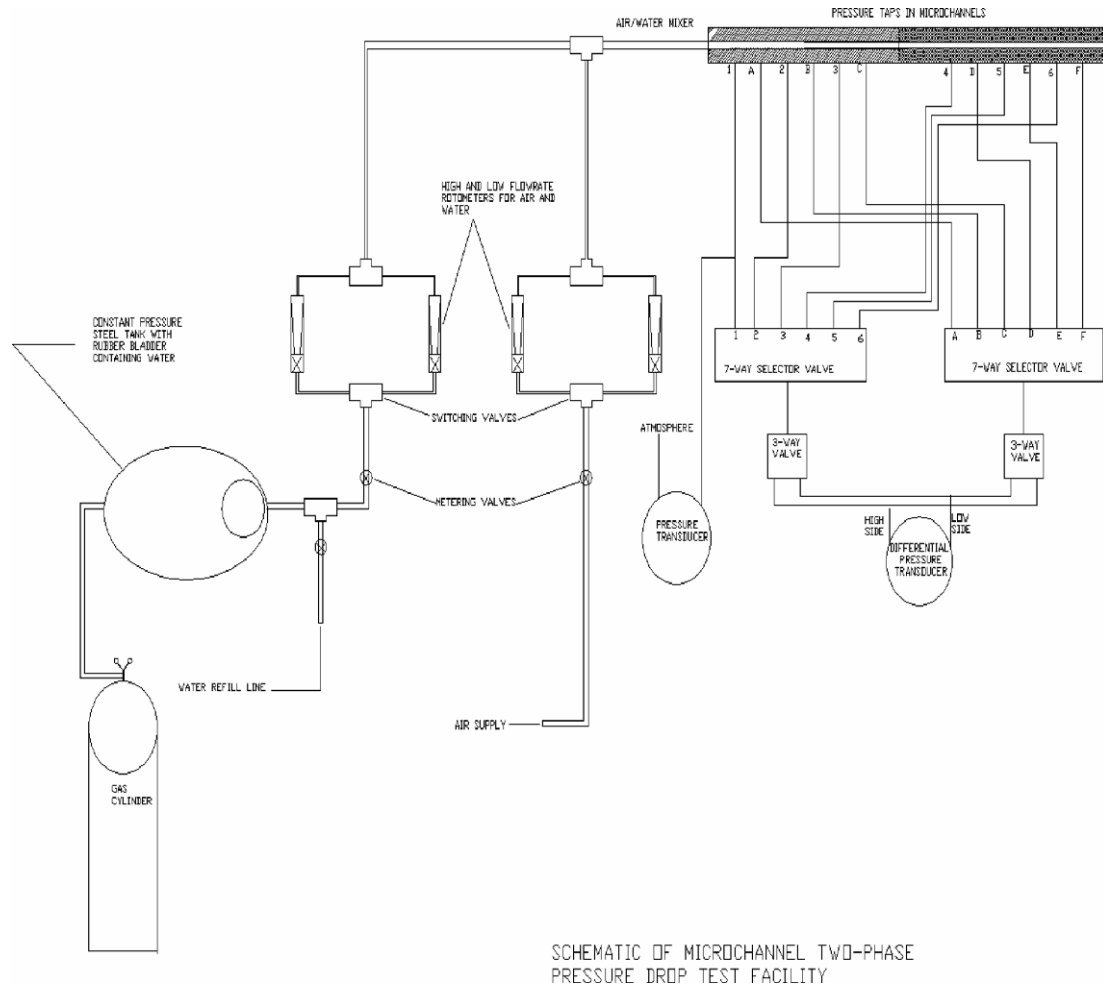


Fig. 1. Schematic of the test facility.

Table 1
Measurement instruments and their accuracy

Description	Manufacturer stated range	Manufacturer stated accuracy
Flow-meter, air	644–2217 cm ³ /min	2%
Flow-meter, water	0.44–20.90 cm ³ /min	2%
Differential pressure transducer	0–37.4 kPa	0.1% cal. range
Differential pressure transducer	0–25 kPa	0.1% cal. range
Total pressure transducer	0–186.8 kPa	0.1% cal. range

area change was found by extrapolating the pressure profiles to the singularity point. Each experiment was repeated at least three times to ensure repeatability. The forthcoming experimental data everywhere represent the average of the repeated tests. More details about the experiments can be found in Chalfi (2007).

3. Results and discussion

The discussion in the forthcoming section will follow the convention displayed in Fig. 4. Thus, channel 1 always refers to the smaller channel; $\Delta P_e = P_{2,1} - P_{2,3}$ (Fig. 4a) refers to the pressure change across the sudden

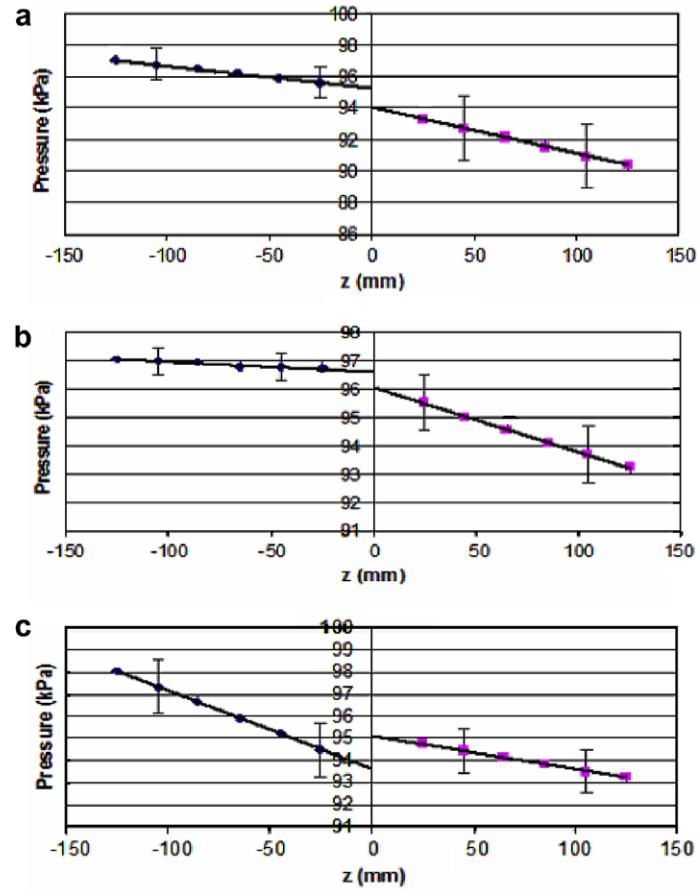


Fig. 2. Typical measured single-phase pressure profiles: (a) water, contraction, $\dot{m} = 0.196$ g/s (b) air, contraction, $\dot{m} = 0.746$ g/s (c) water, expansion, $\dot{m} = 0.256$ g/s.

flow area expansion, and $\Delta P_c = P_{2,3} - P_{2,1}$ (Fig. 4b) represents the pressure change in the sudden flow area contraction.

3.1. Flow area expansion, single-phase flow

Assuming one-dimensional, steady-state and incompressible flow, the total pressure change for a sudden expansion can be represented as:

$$\Delta P_c = \Delta P_{e,R} + \Delta P_{e,I} \tag{1}$$

where subscripts R and I represent the reversible and irreversible components of the pressure change, and

$$\Delta P_{e,R} = -\frac{\langle u_1 \rangle^2}{2} (1 - \sigma^2) \tag{2}$$

$$\Delta P_{e,I} = K_c \frac{1}{2} \rho \frac{\langle u_1 \rangle^2}{2} \tag{3}$$

$$K_c = 1 - 2k_{d1}\sigma + \sigma^2(2k_{d3} - 1) \tag{4}$$

$$\sigma = \frac{A_1}{A_3} \tag{5}$$

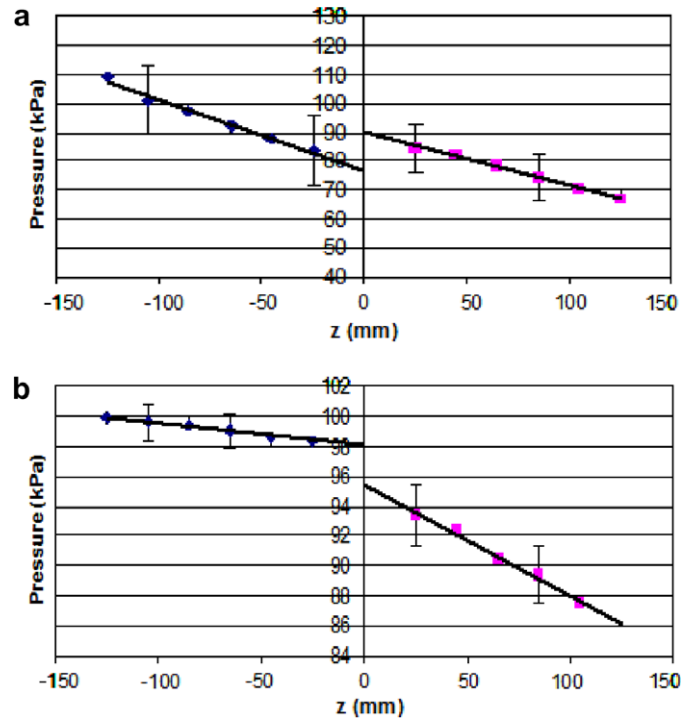


Fig. 3. Typical measured two-phase pressure profiles: (a) expansion, $\dot{m}_L = 0.286$ g/s, $\dot{m}_G = 0.017$ g/s (b) contraction, $\dot{m}_L = 0.256$ g/s, $\dot{m}_G = 0.139$ g/s.

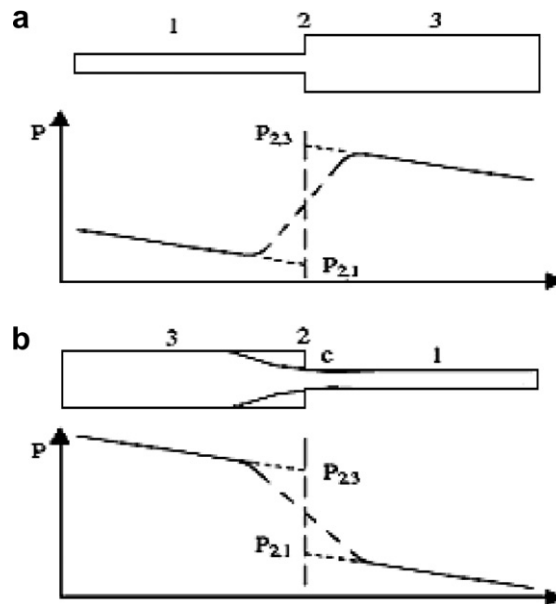


Fig. 4. Definition for pressures: (a) sudden expansion (b) sudden contraction.

In these equations K_e represents the expansion loss coefficient, and k_{d1} and k_{d3} are momentum correction factors for channels 1 and 3 respectively (see Fig. 4a). Furthermore, σ represents the ratio between the smaller and larger flow areas everywhere in this paper. The parameter $\langle u_1 \rangle$ represents the mean velocity in the smaller channel, according to the following definition:

$$\langle \xi \rangle = \frac{1}{A} \int_A \xi da \tag{6}$$

The momentum correction factor is equal to approximately 1.33 for fully-developed laminar flow in a circular channel, and is equal to one when calculations are based on assumed flat velocity profiles. For flat velocity profiles (which is the common practice for the definition of loss coefficients), Eq. (4) leads to the Borda–Carnot relation:

$$K_e = (1 - \sigma)^2 \tag{7}$$

Fig. 5a displays the experimental data for water flow. In this and all other forthcoming figures in this paper the Reynolds number is everywhere based on the smaller channel. The experimental loss coefficients have been found by writing

$$K_e \frac{1}{2} \rho \langle u_1 \rangle^2 = \Delta P_{e, \text{exp}} - \frac{1}{2} \rho \langle u_1 \rangle^2 (\sigma^2 - 1) \tag{8}$$

where $\Delta P_{e, \text{exp}}$ represents the experimentally-measured value of $P_{2,1} - P_{2,3}$ in Fig. 4a. The data evidently represent low Re conditions with $Re \leq 550$. The data, as noted, indicate dependence on Re .

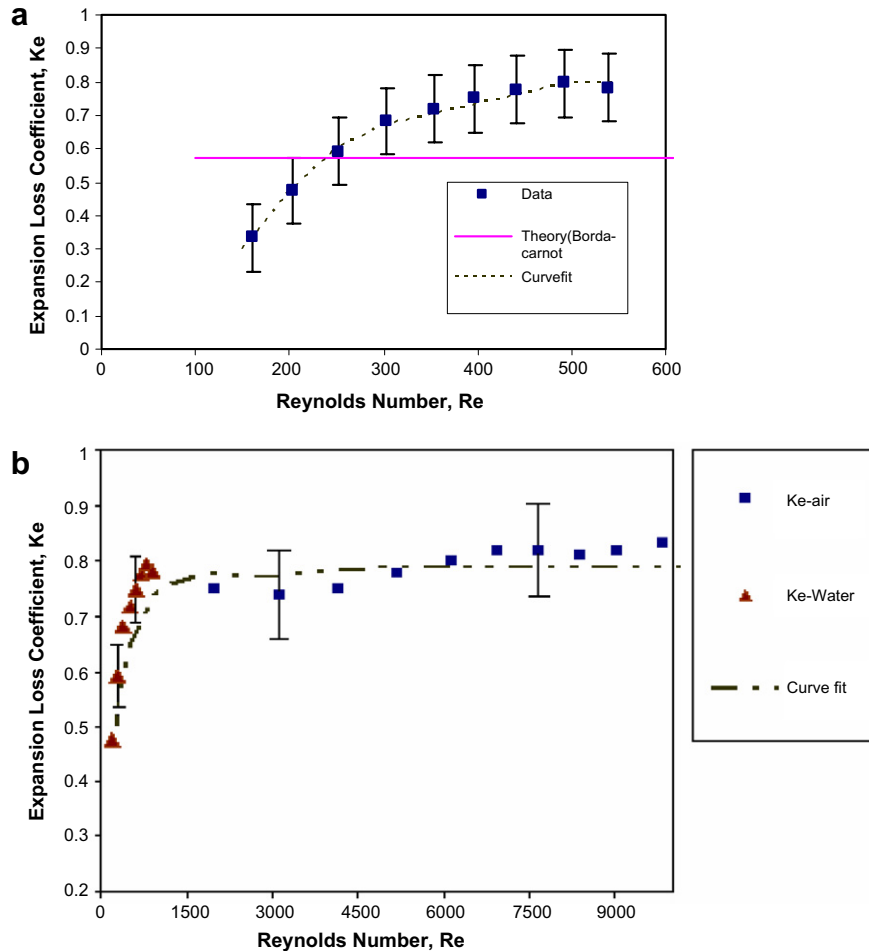


Fig. 5. Expansion loss coefficient in single-phase flow: (a) water (b) water and air.

Fig. 5b depicts the experimental data for air and water. The experimental data for air represent considerably higher Reynolds numbers, and conform to a constant K_e , at least for $Re \geq 5000$. When considered together the data obtained with air and water conform to the following empirical correlations:

$$K_e = 0.80 \quad \text{for } 400 \leq Re \leq 11,000 \quad (9)$$

$$K_e = a + bRe_D + cRe_D^2 \quad \text{for } Re < 400 \quad (10)$$

where $a = -0.2154$, $b = 0.0043$, $c = -5 \times 10^{-6}$.

3.2. Flow area contraction, single-phase flow

For single-phase flow through a sudden flow area contraction, it is usually assumed that the flow up to vena-contracta point (point C in Fig. 4b) is isentropic, and pressure loss takes place during the deceleration of the fluid downstream the vena-contracta point. An analysis based on the assumption that the flow field downstream the vena-contracta point is similar to that in a flow area expansion then gives (Kays, 1950; Abdellall et al., 2005):

$$\Delta P_c = P_{2,3} - P_{2,1} = \Delta P_{c,R} + \Delta P_{c,I} \quad (11)$$

$$\Delta P_{c,R} = \rho \frac{\langle u_1 \rangle^2}{2} (1 - \sigma^2) \quad (12)$$

$$\Delta P_{c,I} = K_c \rho \frac{\langle u_1 \rangle^2}{2} \quad (13)$$

$$K_c = \left(1 - \frac{1}{C_c}\right)^2 \quad (14)$$

where flat velocity profiles have been assumed everywhere. The parameter C_c is the vena-contracta coefficient, and can be estimated from the correlation of Geiger (1964)

$$C_c = 1 - \frac{1 - \sigma}{2.08(1 - \sigma) + 0.5371} \quad (15)$$

The experimental data for air and water are depicted in Fig. 6. The experimental values of K_c were found from

$$K_c \rho \frac{\langle u_1 \rangle^2}{2} = \Delta P_{c, \text{exp}} - \rho \frac{\langle u_1 \rangle^2}{2} (1 - \sigma^2) \quad (16)$$

where $\Delta P_{c, \text{exp}}$ represents the experimentally-measured value of $P_{2,3} - P_{2,1}$ in Fig. 4b. Eq. (14) gives $K_c = 0.38$, and evidently underpredicts most of the data, except at very low Reynolds number. The data, however, could be curvefitted according to

$$K_c = 0.0588 \ln Re + 0.0218 \quad (17)$$

3.3. Flow area expansion, two-phase flow

In two-phase flow usually the total pressure change across a flow area disturbance is rough, because a rigorous and unambiguous breakdown of this pressure change into reversible and irreversible components is difficult. The total pressure drop across a sudden flow area expansion can be represented as (see Fig. 4a):

$$\Delta P_c = G_1^2 \sigma \left(\frac{\sigma}{\rho_3} - \frac{1}{\rho_1} \right) \quad (18)$$

where G_1 is the total (mixture) mass flux in the smallest channel, and subscript 1 and 3 refer to stations 1 and 3 in Fig. 4a. The ‘‘momentum density’’, ρ' is defined as (Lahey and Moody, 1993):

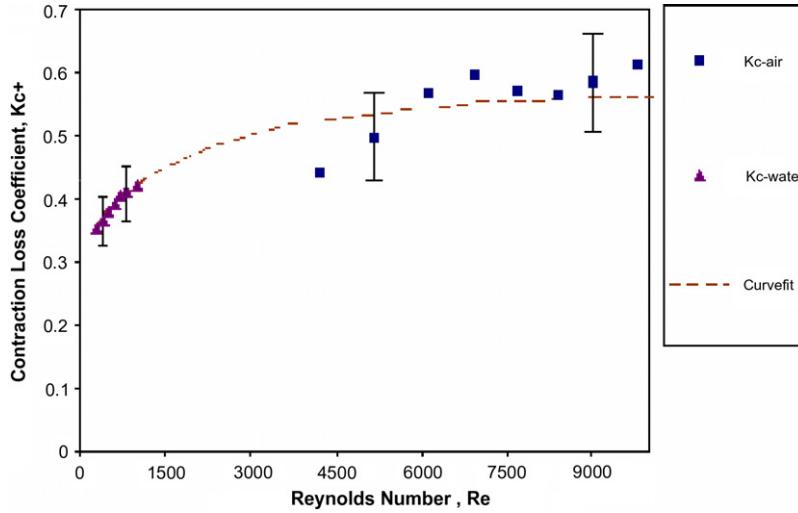


Fig. 6. Contraction loss coefficient in single-phase flow.

$$\rho' = \left[\frac{1 - x^2}{\rho_L(1 - \alpha)} + \frac{x^2}{\alpha\rho_G} \right]^{-1} \quad (19)$$

where x represents quality, and α is the void fraction. Subscripts L and G represent the liquid and gas phases, respectively. If it is assumed that phases are incompressible, and that x and α both remain unchanged during the flow area expansion, Eq. (18) reduces to:

$$\Delta P_c = G_1^2 \sigma \frac{(\sigma - 1)}{\rho'} \quad (20)$$

To apply Eqs. (18) or (20), one evidently needs a void-quality relation, since α is not known. The void-quality relation for one-dimensional flow can be used:

$$\frac{x}{1 - x} = \frac{\rho_G}{\rho_L} S \frac{\alpha}{1 - \alpha} \quad (21)$$

For homogeneous flow $S = 1$.

The experimental sudden flow area expansion data are shown in Fig. 7. Also shown in these figures are the predictions of the homogeneous flow model which over predicts the total pressure change very significantly. The data, however, could be correlated by using the following relation for the slip ratio

$$S = c \left(\frac{\rho_L}{\rho_G} \right)^{1/3} \quad (22)$$

where $c = 0.7$. The above expression with $c = 1$ is in fact the expression of Zivi (1964) for slip flow in annular flow when minimum entropy generation rule is assumed. Alternatively, the data could be correlated using the following Armand-type expression

$$\alpha = C_A \frac{j_G}{j_G + j_L} \quad (23)$$

where j_G and j_L are the gas and liquid superficial velocities, respectively, and $C_A = 0.5$. Fig. 7 indicates that, except for the data depicted in Fig. 7d where the above correlations underpredict the data by up to about 30%, the correlations agree with the data very well.

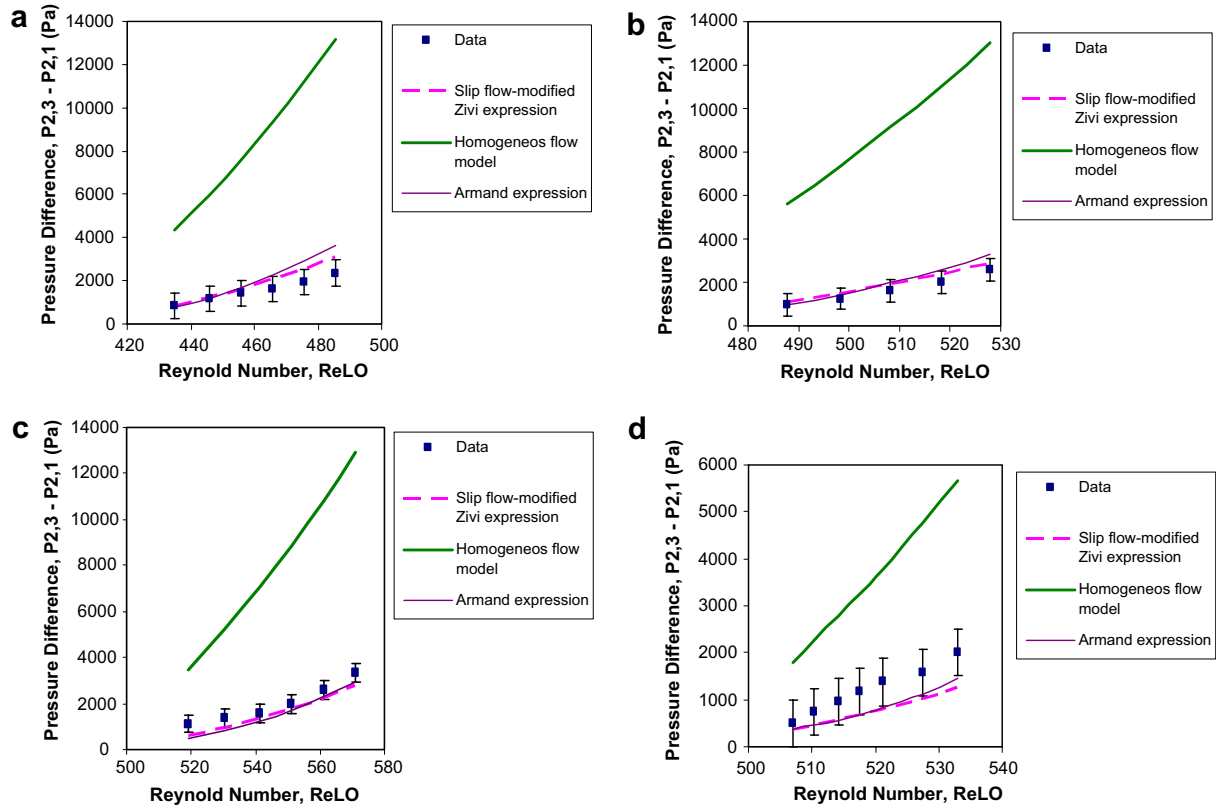


Fig. 7. Two-phase expansion pressure drops: (a) $\dot{m}_L = 0.256$ g/s, $\dot{m}_G = 0.024\text{--}0.057$ g/s (b) $\dot{m}_L = 0.286$ g/s, $\dot{m}_G = 0.027\text{--}0.053$ g/s (c) $\dot{m}_L = 0.317$ g/s, $\dot{m}_G = 0.017\text{--}0.051$ g/s (d) $\dot{m}_L = 0.317$ g/s, $\dot{m}_G = 0.009\text{--}0.026$ g/s.

3.4. Flow area contraction, two-phase flow

Most of the past studies have assumed that the vena-contracta phenomenon occurs in two-phase flow as well, and has the same characteristics as those in single-phase flow (Jansen and Kervinen, 1964; Weisman et al., 1976; Gniglielmi et al., 1986; Al'Ferov and Shul'Zhenko, 1977), and that leads to (see Fig. 4b):

$$\Delta P_c = G_1^2 \left\{ \frac{\bar{\rho}_h}{2} \left(\frac{1}{C_c^2 \rho_{2,1}''} - \frac{\sigma^2}{\rho_3''} \right) + \left(\frac{1}{\rho_1'} - \frac{C_c}{\rho_{2,1}'} \right) \right\} \quad (24)$$

where the numerical subscripts correspond to the locations in Fig. 5b, and ρ'' is defined as:

$$\rho'' = \left[\frac{(1-x)^3}{\rho_L^2 (1-\alpha)^2} + \frac{x^3}{\rho_G^2 \alpha^2} \right]^{-1/2} \quad (25)$$

The parameter $\bar{\rho}_h$ is the homogeneous-flow density found by using properties averaged between points 2 and C (the vena-contracta point). When the two-phases are both assumed to be incompressible, and assuming that x and α both remain unchanged everywhere, Eq. (25) leads to

$$\Delta P_c = G_1^2 \left\{ \frac{\rho_h}{2\rho'^2} \left(\frac{1}{C_c^2} - \sigma^2 \right) + \frac{1}{\rho'} (1 - C_c) \right\} \quad (26)$$

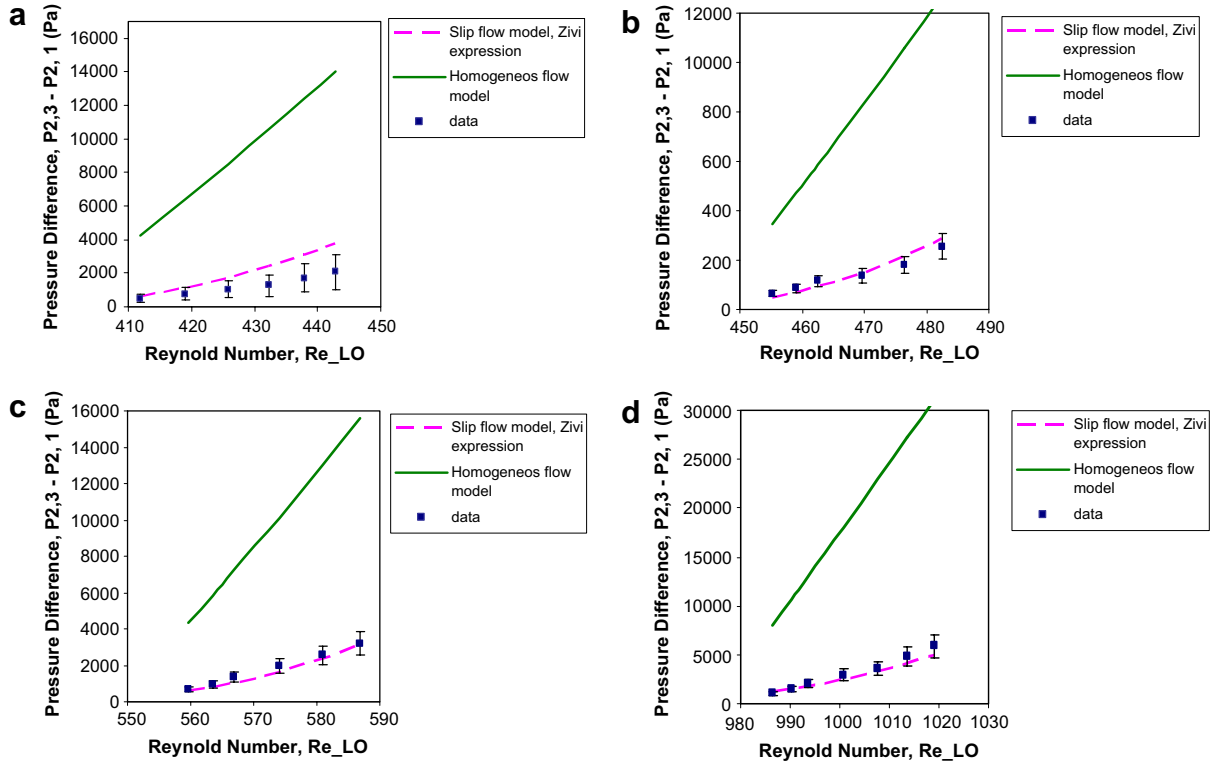


Fig. 8. Two-phase contraction pressure change. All model calculations assume no vena-contracta. (a) $\dot{m}_L = 0.256$ g/s, $\dot{m}_G = 0.009\text{--}0.029$ g/s (b) $\dot{m}_L = 0.286$ g/s, $\dot{m}_G = 0.006\text{--}0.024$ g/s (c) $\dot{m}_L = 0.353$ g/s, $\dot{m}_G = 0.006\text{--}0.024$ g/s (d) $\dot{m}_L = 0.628$ g/s, $\dot{m}_G = 0.006\text{--}0.027$ g/s.

If the flow is assumed to be homogeneous everywhere, then

$$\Delta P_c = \frac{G_1^2}{2\rho_L} \left\{ \left(\frac{1}{C_c} - 1 \right)^2 + (1 - \sigma^2) \right\} \left[1 + x \frac{(\rho_L - \rho_G)}{\rho_L} \right] \quad (27)$$

However, a careful experimental investigation by Schmidt and Friedel (1997) has shown that the vena-contracta phenomenon may actually not occur in two-phase flow at all.

The measured total pressure changes for two-phase flow through the flow area contraction are displayed in Fig. 8, where $Re_{LO} = G_1 D_1 / \mu_L$ is the all-liquid Reynolds number in the smaller channel. The predictions of the homogeneous flow model, when no vena-contracta is assumed (i.e. $C_c = 1$) are also shown in Fig. 8, and indicate that the homogeneous flow model overpredicts the pressure drop very significantly. The predictions of Eq. (26), when $C_c = 1$ is assumed and the expression of Zivi (1964) for the slip [i.e. Eq. (22) with $C_c = 1$] is used, are also shown in Fig. 8. As noted, in this case there is very good agreement between theory and data.

Similar comparison was made between the data and the predictions of the homogeneous flow model, as well as the slip flow model along with Zivi’s slip ratio expression, this time assuming that the vena-contracta phenomenon occurred according to Geiger’s expression [Eq. (15)]. The results (not shown here for brevity) once again showed that the homogeneous model over predicted the pressure drop very significantly everywhere, typically by a factor of five. The slip flow model also over predicted the data consistently, typically by a factor of two.

4. Concluding remarks

Single-phase and two-phase flow pressure drops associated with the flow area expansion and contraction were measured in a system consisting of two capillaries, one with $D = 0.84$ mm, and the other with

$D = 1.6$ mm. Near- atmospheric and room temperature air and distilled water were used. For single-phase flow the loss coefficients were empirically correlated. The two-phase flow data suggest the occurrence of strong velocity slip, and confirm the inadequacy of the one-dimensional homogeneous flow model. The flow area expansion data could be modeled using the one-dimensional slip flow model along with an Armand-type void-quality expression. For flow area contraction a similar model based on the slip ratio expression of Zivi (1964) agreed with the data very well, provided that no vena-contracta was considered.

References

- Abdelall, F.F., Hahn, G., Ghiaasiaan, S.M., Abdel-Khalik, S.I., Jeter, S.M., Yoda, M., Sadowski, D.L., 2005. Pressure drop caused by abrupt flow area changes in small channels. *Exp. Therm. Fluid Sci.* 29, 425–434.
- Al'Feroov, N.S., Shul'Zhenko, Ye.N., 1977. Pressure drops in two-phase flows through local resistances. *Fluid Mech.: Soviet Res.* 6, 20–33.
- Bowers, M.B., Mudawar, I., 1994. High flux boiling in low flow rate, low pressure drop mini-channel and micro-channel heat sinks. *Int. J. Heat Mass Transf.* 37, 321–332.
- Chalfi, T.Y., 2007. Pressure loss associated with flow area change in micro-channels. M.S. Thesis, Georgia Institute of Technology, Atlanta, Georgia.
- Chen, Y., Chang, P., 2005. Condensation of steam in silicon microchannels. *Int. Comm. Heat Mass Transf.* 32, 175–183.
- Chung, P.M.-Y., Kawaji, M., Kawahara, A., Shibata, Y., 2004. Two-phase flow through square and circular microchannel – effects of channel geometry. *J. Fluids Eng.* 126, 546–552.
- Geiger, G.E., 1964. Sudden contraction losses in single and two-phase flow. PhD thesis, University of Pittsburgh, Pittsburgh, Pennsylvania.
- Gnglielmini, G., Lorenzi, A., Muzzio, A., and Sotgia, G., 1986. Two-phase flow pressure drops across sudden area contractions pressure and void fraction profiles, In: *Proc. eighth Int. Heat Transf. Conf.*, vol. 5, pp. 2361–2366.
- Jansen, E., Kervinen, J.A., 1964. Two-phase pressure drop across contraction and expansion, steam-water mixture at 600–1400 psia. Report GEAP-4622, General Electric Company, San Jose, California.
- Kays, W.M., 1950. Loss coefficient for abrupt changes in flow cross-section with low Reynolds number flow in single and multiple tube systems. *Trans. ASME* 72, 1067–1074.
- Lahey Jr., T.R., Moody, F.J., 1993. *The Thermal-Hydraulics of Boiling Water Nuclear Reactors*, second ed. American Nuclear Society, LaGrange Park, Illinois.
- Qu, W., Mudawar, I., 2004. Transport phenomena in two-phase micro-channel heat sinks. *J. Electronic Packaging* 126, 213–224.
- Schmidt, J., Friedel, L., 1997. Two-phase pressure drop across sudden contractions in duct areas. *Int. J. Multiphase Flow* 23, 283–299.
- Triplett, K.A., Ghiaasiaan, S.M., Abdel-Khalik, S.I., LeMouel, A., McCord, N., 1999. Gas-liquid two-phase flow in microchannels. Part II: Void fraction and pressure drop. *Int. J. Multiphase Flow* 25, 395–410.
- Weisman, J., Hussain, A., Harshe, B., 1976. Two-phase pressure drop across abrupt area changes and restrictions. In: *Veziroglu, T.N., Kakac, S. (Eds.), Proceedings of the Two-Phase Flow and Heat Transfer Symposium*, Washington, D.C., pp. 301–303.
- Wu, H.Y., Cheng, P., 2003. Visualization and measurements of periodic boiling in silicon microchannels. *Int. J. Heat Mass Transf.* 46, 2603–2614.
- Yang, C.-Y., Webb, R.L., 1996. Friction pressure drop of R-12 in small hydraulic diameter extruded aluminum tubes with and without micro-fins. *Int. J. Heat Mass Transf.* 39, 801–809.
- Zhang, M., Webb, R.L., 2001. Correlation of two-phase friction for refrigerants in small-diameter tubes. *Exp. Therm. Fluid Sci.* 25, 131–139.
- Zivi, S.M., 1964. Estimation of steady-state steam void-fraction by means of the principle of minimum entropy production. *J. Heat Transf.* 68, 247–252.